THE JOURNAL OF PHYSICAL CHEMISTRY B

Article

pubs.acs.org/JPCB

Thermal Analysis and Raman Spectra of Different Phases of the Ionic Liquid Butyltrimethylammonium Bis(trifluoromethylsulfonyl)imide

Luiz F. O. Faria,[†] Jivaldo R. Matos,[‡] and Mauro C. C. Ribeiro*,[†]

[†]Laboratório de Espectroscopia Molecular, Instituto de Química, Universidade de São Paulo, CP 26077, CEP 05513-970 São Paulo, SP, Brazil

[‡]Laboratório de Análises Térmicas Ivo Giolitto, Instituto de Química, Universidade de São Paulo, CP 26077, CEP 05513-970 São Paulo, SP, Brazil

Supporting Information

ABSTRACT: The ionic liquid butyltrimethylammonium bis(trifluoromethylsulfonyl)imide, $[C_4C_1C_1C_1N][Tf_2N]$, is a glass-forming liquid that exhibits partial crystallization depending on the cooling rate. Differential scanning calorimetry (DSC) indicates crystallization at T_c = 227 K, melting at T_m = 258 K, glass transition at $T_g \sim 191$ K, and also cold crystallization at $T_{cc} \sim 219$ K. Raman spectroscopy shows that the crystalline structure obtained by slow cooling is formed with $[Tf_2N]^-$ in cisoid conformation, whereas $[Tf_2N]^-$ in transoid conformation results from fast cooling. No preferred conformation of the butyl chain of the $[C_4C_1C_1C_1N]^+$ cation is favored by slow or fast cooling of $[C_4C_1C_1C_1N][Tf_2N]$. Low-frequency Raman spectroscopy shows that crystalline domains developing in the supercooled liquid result in a glacial state made of a mixture of crystallites and amorphous phase. However, these crystalline structures obtained by slow cooling or cold crystallization are not the same because anion−cation interactions promote local structures with distinct conformations of the $[Tf_2N]^-$ anion.

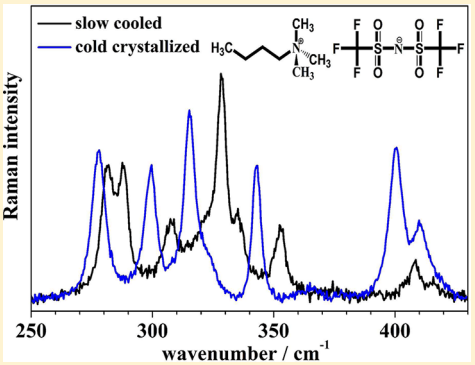

1. INTRODUCTION

A metastable supercooled liquid state is achieved when crystallization is avoided in a liquid that has been cooled below the melting temperature, T_m, of the corresponding crystalline phase. The system reaches an amorphous solid phase as the temperature is further reduced to the glass transition temperature T_g, typically $T_g \sim {}^2/_3 T_m$.[1−4] In contrast to the equilibrium phase transition at T_m, which is uniquely defined for a system in a given pressure, the glass transition is dependent on the thermal history of the sample; for instance, a faster cooling rate gives a higher T_g. Good glass-forming liquids are those systems which are easily supercooled under normal cooling rates, e.g., 10 K min^{-1}, in typical differential scanning calorimetry (DSC) measurements.[1−5] On the other hand, starting from the glassy phase, cold crystallization is eventually observed, i.e., the system crystallizes as the glass is heated to the supercooled liquid phase. This finding suggests that incipient crystal nuclei, whose process of growing has been frustrated, are formed while quenching the liquid into the supercooled range. Instead of microcrystals immersed in the liquid, it has been proposed that frustration between local and global ordering could result in ordered domains whose length scale is only in the range of nanometers.[6−9] Slow relaxation within these ordered regions would be responsible for dynamic heterogeneity in the supercooled liquid. In this physical picture, the so-called glacial state corresponds to a high density amorphous phase resulting from a liquid−liquid phase transition. In the case of crystalline regions of relatively large size, the situation is best described as microcrystallites immersed in an amorphous phase.[10−21] Raman spectroscopy investigations of the glacial state of molecular liquids, e.g., triphenyl phosphite,[11,14,15] *n*-butanol,[18] phenyl salicylate,[21] etc., provided evidence that it is a mixed phase made of microcrystals in a matrix of supercooled liquid. It is worth noting that the glacial state of a given system, for instance, triphenyl phosphite, has been interpreted either as a high density amorphous phase[8] or as a mixed crystal−liquid state.[10,12,13] Both ideas of frustration, giving small ordered clusters and microcrystals in an amorphous phase, highlight the interplay between glass transition and crystallization. However, there is still no consensus whether these domains in metastable phases have the same crystalline structure as that of the thermodynamically stable crystal phase.

Glasses can be obtained from molecular or ionic systems, polymers, metals, or aqueous solutions, pointing to the universality of the phenomenology related to the glass transition. Room temperature molten salts, nowadays simply called ionic liquids, have attracted interest in the past decade because of their wide range of technological applications, for instance, alternative solvents, extraction media, new electrolytes, etc.[22−24] Typical ionic liquids are based on organic cations (imidazolium, piperidinium, pyrrolidinium, ammonium, phosphonium, etc.) and anions such as halides, $[NO_3]^-$,

Received: April 9, 2012
Revised: June 25, 2012
Published: June 27, 2012

dx.doi.org/10.1021/jp3051824 | J. Phys. Chem. B 2012, 116, 9238−9245

$[BF_4]^-$, $[PF_6]^-$, $[CF_3SO_3]^-$, $[(CF_3SO_2)_2N]^-$, etc.[22−25] There is an inherent interest in ionic liquids because the complex molecular structures imply that thermodynamic, structural, and dynamical properties are the result of interplay between intermolecular forces of distinct nature such as Coulombic interactions, van der Waals interactions, hydrogen bonding, etc. Thermophysical characterization has shown that several ionic liquids are good glass-formers exhibiting complex DSC scans, in which glass transition, crystallization, and cold crystallization can be observed.[26−30] For those ionic liquids that are easily supercooled, the glass-transition is usually observed around $T_g \sim 200$ K. On the other hand, ionic liquids that are easily crystallized eventually show polymorphism because several ways of ionic packing are allowed. Raman spectroscopy has been a useful tool to unravel structural differences between distinct crystalline phases resulting from ionic liquids. For instance, ionic liquids based on 1-alkyl-3-methylimidazolium cations might exhibit crystalline phases with a different conformation for the carbon side chain, whereas a mixture of conformers is found in the normal liquid phase.[31] Interestingly, the Raman spectrum in the frequency range appropriate to characterize different conformers (500−700 cm^{-1}) of a crystal of 1-butyl-3-methylimidazolium chloride takes several minutes after melting until the band shape typical of the liquid phase is recovered, suggesting slow cooperative dynamics and structural heterogeneities.[31,32] Complex anions might also exhibit different conformations in the liquid phase, for instance, bis(trifluoromethylsulfonyl)imide ($[Tf_2N]^-$), $[(CF_3SO_2)_2N]^-$, for which Raman spectra in the 250−450 cm^{-1} range suggest $[Tf_2N]^-$ in both transoid and cisoid conformations in ionic liquids.[33−37] Structure determination by X-ray diffraction of single-crystals grown from ionic liquids showed that $[Tf_2N]^-$ can be found in cisoid conformation when the cation is 1,3-dimethylimidazolium[38] or *N*-hexylpyridinium,[39] or in transoid conformation when the cation is 1-butyl-1-methylpyrrolidinium.[40]

In this work, we are concerned with butyltrimethylammonium bis(trifluoromethylsulfonyl)imide, $[C_4C_1C_1C_1N][Tf_2N]$ (see the ionic structures in Figure 1). The choice for

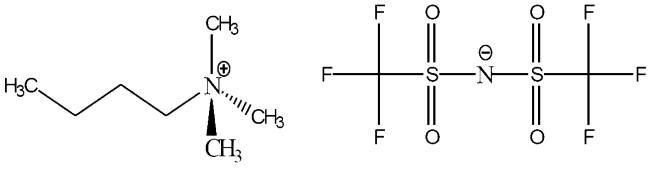

Figure 1. Schematic structures of butyltrimethylammonium, $[C_4C_1C_1C_1N]^+$, and bis(trifluoromethylsulfonyl)imide, $[Tf_2N]^-$.

$[C_4C_1C_1C_1N][Tf_2N]$ relies on the finding that this ionic liquid is easily supercooled, but also partial crystallization is eventually observed while cooling the sample. It turned out that Raman bands assigned to the anion normal modes are good probes of different ionic structures that are obtained as the sample undergoes distinct protocols of cooling and heating. A previous Raman spectroscopy study showed that crystalline phases of 1-ethyl-3-methylimidazolium bis(trifluoromethylsulfonyl)imide are obtained with different conformations of the $[Tf_2N]^-$ anion depending on the cooling rate.[37] In this work, we aim a correlation between macroscopic signatures of different phases given by DSC measurements and microscopic local structures unraveled by Raman spectroscopy. It will be shown that the $[Tf_2N]^-$ anion achieves different conformations when partial crystallization of the supercooled liquid $[C_4C_1C_1C_1N][Tf_2N]$ is obtained by slow cooling or by cold crystallization.

2. EXPERIMENTAL SECTION

The ionic liquid $[C_4C_1C_1C_1N][Tf_2N]$ was purchased from Iolitec and used without further purification. The ionic liquid was dried under high vacuum (below 10^{-5} mbar) for several days. Karl Fischer analysis indicated that water content in the ionic liquid was reduced below 30 ppm.

Thermophysical characterization of $[C_4C_1C_1C_1N][Tf_2N]$ was performed with a differential scanning calorimeter model DTA-50 (Shimadzu) using aluminum pans, hermetically sealed using a sample encapsulating press. Liquid nitrogen was used as a coolant. The sample was first heated above room temperature until 348 K to remove crystal nuclei eventually present in the liquid phase. The sample was slowly cooled at a rate of 1 K min^{-1} and then reheated at 5 K min^{-1}. The temperature was again raised to 348 K to remove any remaining nuclei. Another cycle of cooling at a higher rate of 5 K min^{-1} and heating has been performed. The DSC measurements provide the crystallization temperature, T_c, the glass transition temperature, T_g, the temperature of cold crystallization, T_{cc}, and the melting temperature, T_m. Duplicate measurements were performed to confirm the results.

Raman spectra as a function of temperature were recorded with a Jobin-Yvon T64000 triple monochromator spectrometer equipped with CCD. The spectra were excited with the 647.1 nm line of a mixed argon−krypton Coherent laser, and the spectral resolution was 2.0 cm^{-1}. Raman spectra as a function of temperature were obtained in the usual 90° scattering geometry with no selection of polarization of the scattered radiation. Temperature control was achieved with an Optistat^{DN} cryostat (Oxford Instruments), in which a small amount of sample in a glass tube (3 mm diameter, 40 mm length) allows for cooling the whole sample in a relatively fast rate. Raman spectra have been obtained for partially crystallized samples after slow or fast cooling protocols. First, the ionic liquid was rapidly cooled to 170 K at a rate of 20 K min^{-1} to obtain the glassy state. This fast cooling procedure was followed by stepwise reheating of the sample, allowing for 30 min of equilibrium for each 10 K, until we observed cold crystallization as the sample became opaque. In contrast, the slow cooling procedure started from the normal liquid phase at room temperature followed by stepwise cooling, allowing for 30 min of equilibrium for each 10 K. Following this slow cooling protocol, partial crystallization of the sample was also observed as it became opaque.

3. COMPUTATIONAL DETAILS

Quantum chemistry calculations of the optimized ionic structures and vibrational frequencies were performed using the Gaussian03 package.[41] For comparison purposes, calculations were performed with two levels of theory, density functional theory (DFT) and second-order perturbation theory of Moller−Plessett (MP2). Becke's three-parameter hybrid exchange functional and Lee−Yang−Parr correlation functional (B3LYP)[42,43] were used in the DFT calculations. The basis set used in both DFT and MP2 calculations was 6-311++G(d,p). No imaginary vibrational frequencies were obtained, indicating that the ionic geometry was at the minimum of the potential surface. A scaling factor of 1.082 was used to correct the vibrational frequencies of $[Tf_2N]^-$ calculated by DFT, but no scaling factor was considered for the anion modes calculated by

dx.doi.org/10.1021/jp3051824 | J. Phys. Chem. B 2012, 116, 9238−9245

MP2. The scaling factor was defined by adjusting the calculated value of the most intense anion normal mode to the experimental Raman shift observed at 741 cm^{-1}. Vibrational frequencies of the $[C_4C_1C_1C_1N]^+$ cation were calculated only by DFT level of theory. Scaling factor 1.010 has been used for vibrational frequencies calculated for $[C_4C_1C_1C_1N]^+$ in anti−anti and gauche−anti conformations.

4. RESULTS AND DISCUSSION

A. Thermal Analysis. Figure 2 shows DSC scans of $[C_4C_1C_1C_1N][Tf_2N]$ with two different cooling rates, 1 K

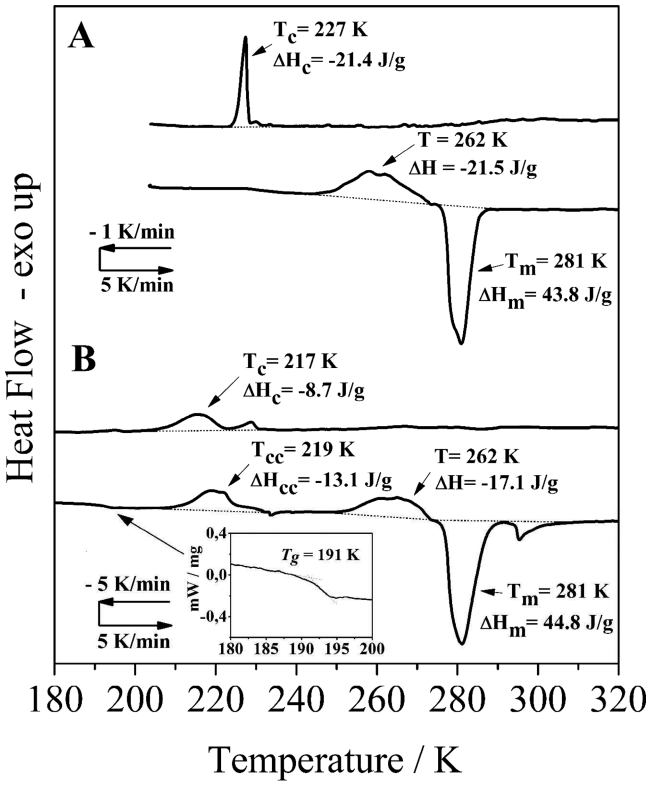

Figure 2. DSC scans of $[C_4C_1C_1C_1N][Tf_2N]$: (A) slow cooling (1.0 K min^{-1}) followed by heating (5.0 K min^{-1}); (B) fast cooling (5.0 K min^{-1}) followed by heating (5.0 K min^{-1}).

min^{-1} (A) and 5.0 K min^{-1} (B). It is clear from Figure 2 that the exothermic peak indicating crystallization obtained with slow cooling (T_c = 227 K) is sharper and more intense than fast cooling (T_c = 217 K). There are small exothermic bumps before crystallization, suggesting that the system undergoes successive attempts at crystallization. The areas of the endothermic peaks indicating melting at T_m = 281 K in both the DSC scans give comparable enthalpies. The DSC scan for the sample that experienced fast cooling exhibits glass transition at T_g= 191 K, which is a typical value for ionic liquids.[26−30] The DSC scan for the fast-cooled sample has another exothermic peak within $T_g < T < T_m$ range that can be assigned to cold crystallization at T_{cc} = 219 K. It should be noted that a broad premelting peak at 262 K precedes the sharp melting peak, as previously found in DSC measurements of other ionic liquids.[30,44−47] Furthermore, the DSC scan of the fast-cooled sample shows a small endothermic peak at 295 K after the main melting peak. DSC measurements of imidazolium ionic liquids using a highly sensitive calorimeter showed that the premelting phenomenon is due to conformational changes in the alkyl chain of the cation in domains where local melting is taking placing.[45−47] The complex thermal behavior of ionic liquids has been called "rhythmic melting and crystallization" and assigned to formation and collapse of polar and nonpolar domains occurring either in the premelting or in the liquid after the melting of the sample.[45−47] In the origin of such complex thermal behavior is the link between phase transition and cooperative conformational changes of the flexible ions.

The comparison of DSC scans in Figure 2 indicates that crystallization of the sample during fast cooling is not as complete as crystallization during slow cooling. Further crystallization of the fast-cooled sample occurs at T_{cc}, i.e., just after the glass is heated above T_g entering the supercooled liquid range. It should be noted that in both the scans the sum of released heat is almost equal to the amount of heat absorbed in the melting process. In the following, Raman spectroscopy will unravel partial crystallization of $[C_4C_1C_1C_1N][Tf_2N]$ and differences in local structures between the samples that experienced slow or fast cooling. The finding of partial crystallization suggests that the supercooled ionic liquid has crystalline domains surrounded by the amorphous phase. Therefore, like several molecular glass-formers, a glacial state made of a mixture of crystallites and supercooled liquid can be obtained for the ionic liquid $[C_4C_1C_1C_1N][Tf_2N]$.

B. Raman Spectra. Optical Kerr effect (OKE) spectroscopy has given important insights on short-time intermolecular dynamics of ionic liquids.[48−55] In OKE spectroscopy, time domain data are Fourier transformed, resulting in an intermolecular vibrational spectrum. Raman and OKE spectroscopies probe polarizability fluctuations, but the corresponding spectra differ by a population factor.[56,57] In the low-frequency Raman spectrum, there is a quasielastic scattering (QES) centered at zero frequency with few wavenumbers of bandwidth due to fast (picosecond) relaxational motions. As temperature drops along the supercooled liquid range into the glassy state, low-frequency Raman spectra exhibit a remarkable decrease in the QES intensity, unraveling the intermolecular vibrational dynamics.[58−62] Thus, in the susceptibility representation, $\chi''(\omega) = I(\omega)/[n(\omega) + 1]$, where $I(\omega)$ is the experimental Raman spectrum and $n(\omega) = [\exp(h\omega/kT) - 1]^{-1}$, depolarized Raman and OKE spectra are comparable.

Figure 3 shows Raman spectra of $[C_4C_1C_1C_1N][Tf_2N]$ in the $\chi''(\omega)$ representation. Raman spectra of glasses exhibit a broad band due to intermolecular vibrational dynamics of an amorphous phase.[58−63] In the case of $[C_4C_1C_1C_1N][Tf_2N]$, the maximum is found at 14 cm^{-1} in the raw Raman spectrum (not shown), and ~20 cm^{-1} in the $\chi''(\omega)$ representation (green line in Figure 3). Because the low-frequency band is due to intermolecular vibrational motions, the peak exhibits a slight shift to higher frequency as the system becomes more rigid with decreasing temperature. The peak position observed in the low-frequency Raman spectrum of $[C_4C_1C_1C_1N][Tf_2N]$ is consistent with data for other ionic liquids.[64,65]

It has been shown that distinct components are buried within the broad spectral feature observed in Raman and OKE spectra of ionic liquids in the frequency range below 100 cm^{-1}.[48−55] Raman and OKE spectra of ionic liquids based on aromatic cations, such as imidazolium and pyridinium derivatives, with the common $[Tf_2N]^-$ anion, exhibit larger contribution from cation motions proper to the large polarizability anisotropy in comparison with nonaromatic cations. In a recent OKE spectroscopy study of monoalkylammonium nitrate ionic

dx.doi.org/10.1021/jp3051824 | J. Phys. Chem. B 2012, 116, 9238−9245

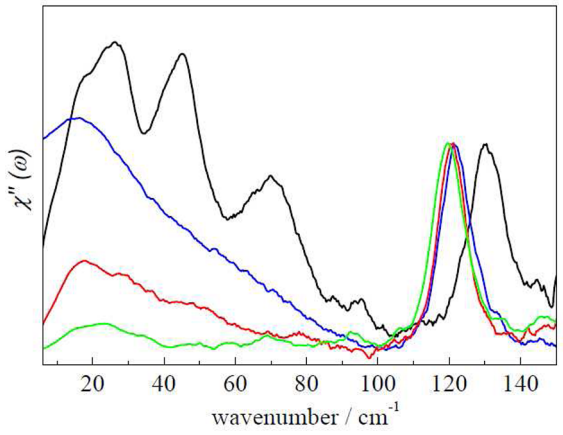

Figure 3. Low-frequency Raman spectra in the susceptibility representation of $[C_4C_1C_1C_1N][Tf_2N]$: liquid (T = 293 K, blue line), glass (T = 170 K, green line), and partially crystallized samples after slow cooling (T = 240 K, black line) and cold crystallization (T = 230 K, red line). The spectra have been normalized by the intensity of $[Tf_2N]^-$ normal mode at 120 cm^{-1}.

liquids,[55] it has been proposed that OKE spectra of these systems are sensitive only to nitrate dynamics because of its large polarizability anisotropy. In contrast, in the OKE spectrum of $[C_4C_2C_2C_2N][Tf_2N]$, which is an ionic liquid very related to the system investigated in this work, it was considered that both the cation and the anion species contribute to the interionic vibrational dynamics proper to similar polarizability anisotropies.[51] A previous work comparing Raman spectra of ionic liquids based on the $[Tf_2N]^-$ anion with aromatic and nonaromatic cations showed that a band with maximum close to 100 cm^{-1}, assigned to librational motions of the aromatic cation, is consistently absent in the Raman spectrum of $[C_4C_1C_1C_1N][Tf_2N]$.[65] Accordingly, the overall band shape of OKE and low-frequency Raman spectra of nonaromatic ionic liquids are less broad than corresponding data for aromatic ionic liquids.[51,54,64,65]

Low-frequency Raman spectroscopy has been useful to show that the glacial state of several molecular liquids is made of a mixture of small crystals immersed in the supercooled liquid phase.[11,15,18,21] In the case of a mixture of microcrystals and supercooled liquid, it is eventually possible to observe sharp bands of phonon modes characteristic of a crystalline phase on the top of the broad band characteristic of the amorphous phase. Figure 3 indicates that is the situation when partial crystallization of the sample was observed by slow cooling of $[C_4C_1C_1C_1N][Tf_2N]$. Similar low-frequency Raman spectra have been obtained for the glacial state of several molecular liquids, for instance, triphenyl phosphite,[11] n-butanol,[18] and phenyl salicylate.[21] In contrast to the band shape of the glassy phase, the Raman spectrum of the slowly cooled sample exhibits bands arising from crystalline domains in the matrix of the supercooled liquid. Of course, the crystallization of $[C_4C_1C_1C_1N][Tf_2N]$ was not complete, because the Raman spectrum does not exhibit only the very sharp peaks typical of a crystal. In other words, the low-frequency Raman spectrum of a partially crystallized sample of $[C_4C_1C_1C_1N][Tf_2N]$ is a superposition of patterns typical of amorphous and crystalline phases even for the slowly cooled sample. It is worth noting that the Raman spectrum of the sample after cold crystallization is different from Raman spectra of the glassy phase and the slowly cooled sample, either in the low-frequency range or in the high-frequency range, as discussed in the following. It should be noted that the sharp peak seen at 120 cm^{-1} in Figure 3 is an internal mode of the $[Tf_2N]^-$ anion, which is assigned as bending of the CSN angle by quantum chemistry calculations. The vibrational frequency of this normal mode is shifted to 130 cm^{-1} in the slowly cooled sample. The calculations indicate that such a difference in vibrational frequency for this mode is characteristic of $[Tf_2N]^-$ in transoid or cisoid conformation, respectively. This is a first indication that the crystalline domains resulting from slow cooling or cold crystallization have different local structures, as clearly seen in the following for other spectral ranges more appropriate to discriminate between different conformations of the $[Tf_2N]^-$ anion.

The spectral range that has been extensively used to characterize transoid and cisoid conformations of $[Tf_2N]^-$ is shown in Figure 4 for $[C_4C_1C_1C_1N][Tf_2N]$.[33−37] It is clear

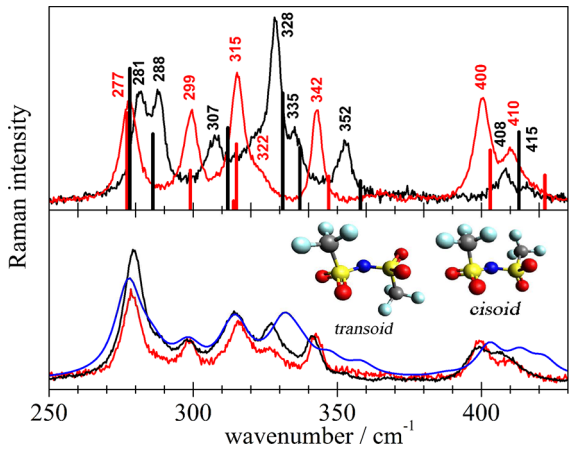

Figure 4. Top panel: Raman spectra of partially crystallized samples of $[C_4C_1C_1C_1N][Tf_2N]$ after slow cooling (T = 240 K, black line) and cold crystallization (T = 230 K, red line). Vertical lines give wavenumbers and relative intensities of Raman bands calculated by DFT level of theory for $[Tf_2N]^-$ in transoid (red lines) and cisoid (black lines) conformations. Bottom panel: Raman spectra of liquid (T = 293 K, black line) and glassy (T = 170 K, red line) phases of $[C_4C_1C_1C_1N][Tf_2N]$. The blue line is the Raman spectrum simulated by summing DFT data for $[Tf_2N]^-$ in transoid and cisoid conformations using Lorentzian bandshapes with 10 cm^{-1} bandwidths.

from Figure 4 that Raman spectra in the 250−450 cm^{-1} range are very different for samples after slow cooling or after cold crystallization (black and red lines in top panel). A previous investigation of ionic liquids based on quaternary ammonium cations and $[Tf_2N]^-$ anion suggested that crystals with distinct $[Tf_2N]^-$ conformers could be obtained depending on the cooling rate,[66] although no clear difference is seen in the corresponding Raman spectra shown in Figure 1 of ref 66. Table 1 compares vibrational frequencies observed in this frequency range with those calculated by DFT and MP2 methods for $[Tf_2N]^-$ in transoid and cisoid conformations. The peak positions and relative intensities calculated by DFT are also indicated in Figure 4. We have not found previous calculations of the $[Tf_2N]^-$ vibrational frequencies by MP2 level of theory, but Table 1 shows that MP2 results are similar to DFT. (A full list of Raman shifts and relative intensities calculated by quantum chemistry are provided as Supporting Information.) Vibrational modes in this spectral range have been assigned to twisting, rocking, wagging, and torsion modes of the SO_2 and CF_3 groups.[33−37] Among the vibrational

dx.doi.org/10.1021/jp3051824 | J. Phys. Chem. B 2012, 116, 9238−9245

Table 1. Vibrational Frequencies (cm^{-1}) of $[Tf_2N]^-$ Normal Modes Observed in the 250−450 cm^{-1} Range of Raman Spectra of $[C_4C_1C_1C_1N][Tf_2N]$[a]

	transoid $[Tf_2N]^-$		cisoid $[Tf_2N]^-$	
frequency	DFT	MP2	DFT	MP2
277[b]	277 (10.5)	275 (7.9)	–	–
281[c]	–	–	278 (7.8)	277 (5.9)
288[c]	–	–	286 (3.9)	282 (2.8)
299[b]	299 (3.7)	287 (3.6)		
307[c]	–	–	312 (4.3)	302 (4.1)
315[b]	315 (6.8)	306 (5.9)	–	–
322[b]	314 (0.02)	315 (0.02)	–	–
328[c]	–	–	331 (6.3)	323 (6.7)
335[c]	–	–	337 (3.1)	328 (2.8)
342[b]	347 (3.0)	336 (3.5)	–	–
352[c]	–	–	358 (1.2)	346 (1.9)
400[b]	403 (6.1)	390 (5.1)	–	–
408[c]	–	–	413 (4.1)	397 (3.6)
410[b]	422 (3.1)	406 (3.0)	–	–
415[c]	–	–	455 (1.2)	423 (1.3)

[a]Wavenumbers and relative intensities (in parentheses) calculated by DFT and MP2 levels of theory are given for transoid and cisoid conformers. [b]Cold-crystallized sample, T = 230 K. [c]Slowly cooled sample, T = 240 K.

frequencies listed in Table 1, the more characteristic features of each conformer of $[Tf_2N]^-$ is the 328 cm^{-1} band as a signature of the cisoid conformer, and 315 and 342 cm^{-1} bands as signatures of the transoid conformer. Eigenvectors of these three vibrational modes obtained by DFT calculations are shown in Figure 5, indicating that the assignment of these modes is rather complex because several atoms are involved in the normal coordinate. Nevertheless, it is relatively easy to assign the Raman spectrum of the cold-crystallized sample of $[C_4C_1C_1C_1N][Tf_2N]$ to dominance of $[Tf_2N]^-$ in transoid conformation. In contrast, the slowly cooled sample gives crystalline structures with $[Tf_2N]^-$ in cisoid conformation. Raman spectra of normal liquid and glassy phases of $[C_4C_1C_1C_1N][Tf_2N]$ shown in the bottom panel of Figure 4 are similar to each other but different from the partially crystallized samples. The spectrum shown as a blue line is a superposition of DFT-calculated spectra of transoid and cisoid $[Tf_2N]^-$, with 40% contribution of the latter, assuming Lorentzian shapes of 10 cm^{-1} bandwidth. Thus, Raman spectra of the normal liquid and glassy phases correspond to a mixture of $[Tf_2N]^-$ conformers, because the energy of the cisoid conformer is only ~3.5 kJ/mol higher than that of the transoid conformer.[35,37]

It would be interesting to search for distinct conformations of the butyl chain of $[C_4C_1C_1C_1N]^+$ when partial crystallization of $[C_4C_1C_1C_1N][Tf_2N]$ is obtained after fast or slow cooling. Figure 6 shows Raman spectra of different phases of $[C_4C_1C_1C_1N][Tf_2N]$ in the 500−750 cm^{-1} and 850−1100 cm^{-1} ranges which can be used to characterize the cation conformation. The 500−750 cm^{-1} range is usually considered to discriminate between anti−anti and gauche−anti conformers of ionic liquids based on 1-butyl-3-methylimidazolium cations.[31] However, there are Raman bands of $[Tf_2N]^-$ in this spectral range (see the 530−620 cm^{-1} range marked in Figure 6). Anion Raman bands in this range also indicate different conformations of $[Tf_2N]^-$ in the crystallites obtained by slow or fast cooling, whereas the liquid and the glassy phases

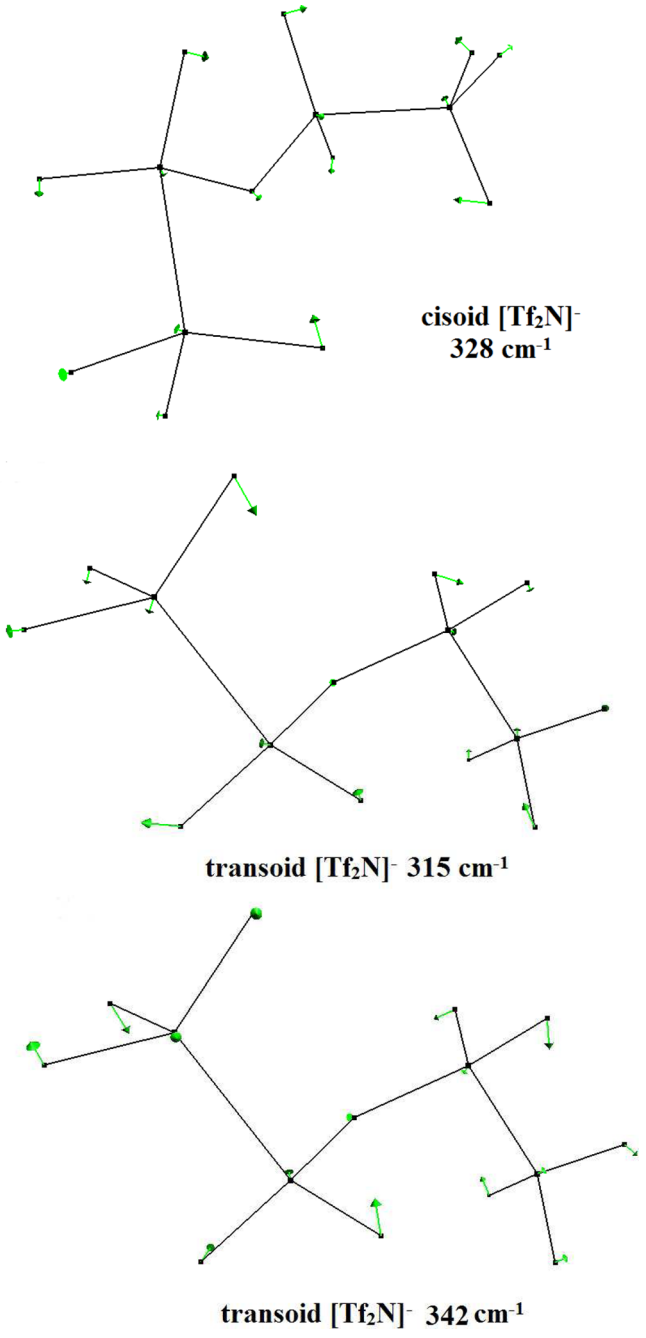

Figure 5. Atomic displacements of some eigenvectors calculated by DFT level of theory for characteristic vibrational modes of $[Tf_2N]^-$ in cisoid (328 cm^{-1}) and transoid (315 and 342 cm^{-1}) conformations.

contain a mixture of conformers. The advantage of the 850−1100 cm^{-1} range is that it is free of $[Tf_2N]^-$ bands. The comparison between Raman spectra of partially crystallized samples after slow or fast cooling (top panel of Figure 6) indicate only small differences in peak positions and relative intensities of $[C_4C_1C_1C_1N]^+$ bands. There is no clear indication that a given conformer of $[C_4C_1C_1C_1N]^+$ dominates the crystalline domains resulting from different thermal histories. The Raman spectra suggest that the mixture of anti−anti and gauche−anti conformers of $[C_4C_1C_1C_1N]^+$ in the liquid phase remains in the glassy and partially crystallized phases of $[C_4C_1C_1C_1N][Tf_2N]$.

dx.doi.org/10.1021/jp3051824 | J. Phys. Chem. B 2012, 116, 9238−9245

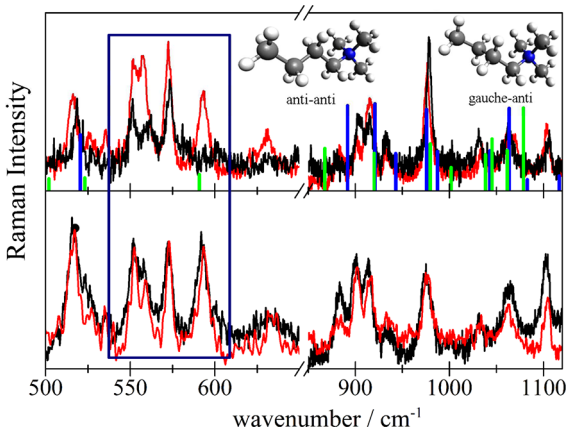

Figure 6. Top panel: Raman spectra of partially crystallized samples of $[C_4C_1C_1C_1N][Tf_2N]$ after slow cooling (T = 240 K, black line) and cold crystallization (T = 230 K, red line). Vertical lines give wavenumbers and relative intensities of Raman bands calculated by DFT level of theory for $[C_4C_1C_1C_1N]^+$ in anti−anti (blue lines) and gauche−anti (green lines) conformations. Raman bands in the 530 < ω < 620 cm^{-1} range inside the blue square belong to $[Tf_2N]^-$ normal modes. Bottom panel: Raman spectra of liquid (T = 293 K, black line) and glassy (T = 170 K, red line) phases of $[C_4C_1C_1C_1N][Tf_2N]$.

Evidence from neutron and X-ray scattering spectroscopy and computer simulations suggests that ionic liquids have nanoscale heterogeneities due to coexisting polar and nonpolar domains.[27,53,67−73] Polar domains result from anions interacting with the polar part of cations, whereas van der Waals interactions between side carbon chains result in nonpolar domains. Neutron diffraction measurements on protic ionic liquids based on monoalkylammonium cations and the nitrate anion indicated nonpolar domains due to aggregation of alkyl chains of neighboring cations, and polar domains made by the ammonium group interacting with NO_3^- anions by eletrostatic attractions and hydrogen bonds.[74,75] In this work, we found that anion conformation is optimized in the more polar domain of the ionic liquid during slow crystallization of $[C_4C_1C_1C_1N][Tf_2N]$, whereas a mixture of carbon chain conformations remains in nonpolar domains. This is an interesting finding in light of recent studies indicating that separation of polar/nonpolar domains is not as well-defined in nonaromatic as it is in aromatic ionic liquids with similar length of the carbon chain and the $[Tf_2N]^-$ anion.[67,72,73,76,77] For instance, whereas ionic liquids based on 1-butyl-3-methylimidazolium show a small wave-vector peak in the static structure factor indicating an intermediate-range order, such a feature has been not found in X-ray scattering investigation of $[C_4C_4C_4C_1N][Tf_2N]$.[76] In nonaromatic ionic liquids, evidence of microheterogeneity appears for cations of longer alkyl chains.[73] Even though polar/nonpolar segregation might not be clearly developed in $[C_4C_1C_1C_1N][Tf_2N]$, the Raman spectra obtained in this work clearly show conformational change to cisoid $[Tf_2N]^-$, but not preferred conformation of the butyl chain of $[C_4C_1C_1C_1N]^+$, during slow cooling. Thus, local anion−cation interactions are optimized in the more polar part of the crystalline structures, while the carbon chains are allowed to keep the mixture of conformers characteristic of the liquid phase during slow cooling of $[C_4C_1C_1C_1N][Tf_2N]$. Previous heat capacity measurements of ionic liquids based on 1-alkyl-3-methylimidazolium cations suggested an analogous physical picture.[78] An inflection point has been found in heat capacity curves, $C_P(T)$, at $T \sim 230$ K in the case of imidazolium ionic liquids containing the $[Tf_2N]^-$ anion. Those anomalies in $C_P(T)$ have been assigned to formation of metastable crystals resulting from distinct $[Tf_2N]^-$ conformers, rather than imidazolium conformers.[78] On the other hand, by heating ionic liquids from a glassy phase at very low temperature, neutron scattering spectroscopy showed sequential triggering of dynamics, starting by conformational motions of the carbon chains before ionic diffusion takes place at high temperature.[27]

It is remarkable that crystalline domains obtained by slow cooling of $[C_4C_1C_1C_1N][Tf_2N]$ are being formed with $[Tf_2N]^-$ in cisoid conformation, because it is more usual crystallization in transoid conformation when the counterion is a large cation. The $[Tf_2N]^-$ anion usually tends to a cisoid conformation when the neighboring cation is a small species such as alkali metal cations,[79,80] so that $[Tf_2N]^-$ is relatively strong coordinated to the cation. A typical ionic liquid forming cation whose crystal structure have been found with $[Tf_2N]^-$ in cisoid conformation is 1,2-dimethylimidazolium, $[C_1C_1Im]^+$.[38] Structure determination of single crystal $[C_1C_1Im][Tf_2N]$ indicated that the cisoid conformation of $[Tf_2N]^-$ is stabilized by several hydrogen bonds to neighboring $[C_1C_1Im]^+$ cations. Therefore, we assigned the partial crystallization of slowly cooled $[C_4C_1C_1C_1N][Tf_2N]$ with $[Tf_2N]^-$ in cisoid conformation as the consequence of hydrogen bonding of anion to several methyl groups of nearest neighbors $[C_4C_1C_1C_1N]^+$ cations.

Whereas slow cooling of $[C_4C_1C_1C_1N][Tf_2N]$ produced crystalline structures with cisoid conformation of $[Tf_2N]^-$, the crystallites formed by cold crystallization are such that the $[Tf_2N]^-$ anion assumes the transoid conformation. The Raman spectra shown in Figure 4 for liquid and glassy phases of $[C_4C_1C_1C_1N][Tf_2N]$ suggest that the relative population of transoid conformer is higher than cisoid conformer in the amorphous phases. In fact, dominance of transoid over cisoid conformers of $[Tf_2N]^-$ in the normal liquid phase has been found in previous Raman spectroscopy investigations of ionic liquids.[34,37] Finding transoid conformation during cold crystallization indicates that crystal nuclei have been formed during fast cooling of the supercooled liquid with the dominant transoid conformation. These nuclei grow while reheating the glass, but this is not the structure that should be found in a better formed crystal during slow cooling of $[C_4C_1C_1C_1N][Tf_2N]$ for which $[Tf_2N]^-$ is in cisoid conformation. Therefore, Raman spectroscopy indicates a metastable crystalline structure obtained after fast cooling that is different from the structure of crystal obtained by slow cooling, respectively, with transoid or cisoid conformers of the $[Tf_2N]^-$ anion. Conversion between $[Tf_2N]^-$ conformers is such a slow dynamic process most probably because it depends on collective rearrangements, as previously proposed for the conformational changes of the long alkyl chain of cations during melting of 1-butyl-3-methylimidazolium chloride,[32] and might contribute to the glass-forming ability of $[C_4C_1C_1C_1N][Tf_2N]$.

5. CONCLUSIONS

A relatively small change on cooling rate (1.0 and 5.0 K min^{-1}) is enough to give very different DSC scans for $[C_4C_1C_1C_1N][Tf_2N]$. Partial crystallization along the fast-cooling protocol is followed by cold crystallization as the glass is reheated to the supercooled liquid phase. It is not clear only from DSC measurements that different crystalline structures are produced following fast or slow cooling. Raman spectroscopy, on the other hand, provides clear indication that fast or slow cooling

dx.doi.org/10.1021/jp3051824 | J. Phys. Chem. B 2012, 116, 9238−9245

give crystallites with $[Tf_2N]^-$ in transoid or cisoid conformation, respectively. Crystallization is only partial in both the protocols of cooling, since Raman spectra in the low-frequency range exhibit superposition of a broad band characteristic of amorphous phase and sharp peaks characteristic of lattice vibrations of crystalline phase. Such a mixture of crystallites immersed in a supercooled liquid characterizes a glacial state of $[C_4C_1C_1C_1N][Tf_2N]$. Local structures that are optimized during slow cooling select a preferred configuration for $[Tf_2N]^-$, namely the cisoid conformer, while a mixture of conformations remain for the butyl chain of $[C_4C_1C_1C_1N]^+$. These conformational changes of $[Tf_2N]^-$ must imply collective rearrangements, so that faster cooling rates produce crystalline structures with ions in the conformations more similar to those already existent in the supercooled liquid. This partial crystallization does not produce crystals of $[C_4C_1C_1C_1N][Tf_2N]$ with the more ideal structure for which the $[Tf_2N]^-$ should be in cisoid conformation. The glass-forming ability of $[C_4C_1C_1C_1N][Tf_2N]$ is reasonable in this scenario, because the slow collective dynamics hinders crystallization.

■ ASSOCIATED CONTENT

Supporting Information

Vibrational frequencies and relative Raman intensities of normal modes of $[Tf_2N]^-$ and $[C_4C_1C_1C_1N]^+$ calculated by DFT and MP2 levels of theory. This information is free of charge via the Internet at http://pubs.acs.org.

■ AUTHOR INFORMATION

Corresponding Author

*E-mail: mccribei@iq.usp.br.

Notes

The authors declare no competing financial interest.

■ ACKNOWLEDGMENTS

The authors are indebted to FAPESP and CNPq for financial support.

■ REFERENCES

(1) Doremus, R. H. *Glass Science*; John Wiley & Sons, New York, 1994.
(2) Lubchenko, V.; Wolynes, P. G. *Annu. Rev. Phys. Chem.* **2007**, *58*, 235−266.
(3) Greaves, G. N.; Sen, S. *Adv. Phys.* **2007**, *56*, 1−166.
(4) Debenedetti, P. G.; Stillinger, F. H. *Nature* **2001**, *410*, 259−267.
(5) Angell, C. A.; Ngai, K. L.; McKenna, G. B.; McMillan, P. F.; Martin, S. W. *J. Appl. Phys.* **2000**, *88*, 3113−3157.
(6) Takahashi, Y.; Osada, M.; Masai, H.; Fujiwara, T. *Phys. Rev. B: Condens. Matter Mater. Phys.* **2009**, *79*, 214204-1−214204-5.
(7) Shintani, H.; Tanaka, H. *Nat. Phys.* **2006**, *2*, 200−206.
(8) Kurita, R.; Tanaka, H. *Science* **2004**, *306*, 845−848.
(9) Kobayashi, M.; Tanaka, H. *J. Phys. Chem. B* **2011**, *115*, 14077−14090.
(10) Kivelson, D.; Tarjus, G. *J. Non-Cryst. Solids* **2002**, *307*, 630−636.
(11) Guinet, Y.; Denicourt, T.; Hedoux, A.; Descamps, M. *J. Mol. Struct.* **2003**, *651*, 507−517.
(12) Tarjus, G.; Alba-Simionesco, C.; Grousson, M.; Viot, P.; Kivelson, D. *J. Phys.: Condens. Matter* **2003**, *15*, S1077−S1084.
(13) Hedoux, A.; Guinet, Y.; Foulon, M.; Descamps, M. *J. Chem. Phys.* **2002**, *116*, 9374−9382.
(14) Hedoux, A.; Guinet, Y.; Descamps, M.; Lefebvre, J. *Phase Transit.* **2003**, *76*, 831−836.
(15) Hedoux, A.; Guinet, Y.; Descamps, M.; Hernandez, O.; Derollez, P.; Dianoux, A. J.; Foulon, M.; Lefebvre, J. *J. Non-Cryst. Solids* **2002**, *307*, 637−643.
(16) Hedoux, A.; Dore, J.; Guinet, Y.; Bellissent-Funel, M. C.; Prevost, D.; Descamps, M.; Grandjean, D. *Phys. Chem. Chem. Phys.* **2002**, *4*, 5644−5648.
(17) Hedoux, A.; Denicourt, T.; Guinet, Y.; Carpentier, L.; Descamps, M. *Solid State Commun.* **2002**, *122*, 373−378.
(18) Wypych, A.; Guinet, Y.; Hedoux, A. *Phys. Rev. B* **2007**, *76* (144202), 1−6.
(19) Shmyt'ko, I. M.; Jimenez-Rioboo, R. J.; Hassaine, M.; Ramos, M. A. *J. Phys-Condens. Mat.* **2010**, *22* (195102), 1−9.
(20) Krivchikov, A. I.; Hassaine, M.; Sharapova, I. V.; Korolyuk, O. A.; Jimenez-Rioboo, R. J.; Ramos, M. A. *J. Non-Cryst. Solids* **2011**, *357*, 524−529.
(21) Baran, J.; Davydova, N. A.; Drozd, M. *J. Phys.: Condens. Matter* **2010**, *22* (155108), 1−8.
(22) Plechkova, N. V.; Seddon, K. R. *Chem. Soc. Rev.* **2008**, *37*, 123−150.
(23) Torimoto, T.; Tsuda, T.; Okazaki, K.; Kuwabata, S. *Adv. Mater.* **2010**, *22*, 1196−1221.
(24) Weingärtner, H. *Angew. Chem., Int. Ed.* **2008**, *47*, 654−670.
(25) Mudring, A. V. *Aust. J. Chem.* **2010**, *63*, 544−564.
(26) Hagiwara, R.; Ito, Y. *J. Fluorine Chem.* **2000**, *105*, 221−227.
(27) Triolo, A.; Mandanici, A.; Russina, O.; Rodriguez-Mora, V.; Cutroni, M.; Hardacre, C.; Nieuwenhuyzen, M.; Bleif, H. J.; Keller, L.; Ramos, M. A. *J. Phys. Chem. B* **2006**, *110*, 21357−21364.
(28) Nishikawa, K.; Wang, S. L.; Katayanagi, H.; Hayashi, S.; Hamaguchi, H. O.; Koga, Y.; Tozaki, K. I. *J. Phys. Chem. B* **2007**, *111*, 4894−4900.
(29) Xu, W.; Cooper, E. I.; Angell, C. A. *J. Phys. Chem. B* **2003**, *107*, 6170−6178.
(30) Castner, E. W.; Wishart, J. F.; Shirota, H. *Acc. Chem. Res.* **2007**, *40*, 1217−1227.
(31) Berg, R. W. *Monatsh. Chem.* **2007**, *138*, 1045−1075.
(32) Okajima, H.; Hamaguchi, H.-o. *Chem. Lett.* **2011**, *40*, 1308−1309.
(33) Herstedt, M.; Smirnov, M.; Johansson, P.; Chami, M.; Grondin, J.; Servant, L.; Lassegues, J. C. *J. Raman Spectrosc.* **2005**, *36*, 762−770.
(34) Martinelli, A.; Matic, A.; Johansson, P.; Jacobsson, P.; Borjesson, L.; Fernicola, A.; Panero, S.; Scrosati, B.; Ohno, H. *J. Raman Spectrosc.* **2011**, *42*, 522−528.
(35) Fujii, K.; Fujimori, T.; Takamuku, T.; Kanzaki, R.; Umebayashi, Y.; Ishiguro, S. I. *J. Phys. Chem. B* **2006**, *110*, 8179−8183.
(36) Rey, I.; Johansson, P.; Lindgren, J.; Lassegues, J. C.; Grondin, J.; Servant, L. *J. Phys. Chem. A* **1998**, *102*, 3249−3258.
(37) Lassegues, J. C.; Grondin, J.; Holomb, R.; Johansson, P. *J. Raman Spectrosc.* **2007**, *38*, 551−558.
(38) Holbrey, J. D.; Reichert, W. M.; Rogers, R. D. *Dalton Trans.* **2004**, 2267−2271.
(39) Choudhury, A. R.; Winterton, N.; Steiner, A.; Cooper, A. I.; Johnson, K. A. *J. Am. Chem. Soc.* **2005**, *127*, 16792−16793.
(40) Stefan, C. S.; Lemordant, D.; Biensan, P.; Siret, C.; Claude-Montigny, B. *J. Therm. Anal. Calorim.* **2010**, *102*, 685−693.
(41) Frisch, M. J.; Trucks, G. W.; Schlegel, H. B.; Scuseria, G. E.; Robb, M. A.; Cheeseman, J. R.; Montgomery, J. A.; Vreven, T.; Kudin, K. N.; Burant, J. C. et al. *Gaussian03W*, Wallingford, CT, 2004.
(42) Becke, A. D. *J. Chem. Phys.* **1993**, *98*, 1372−1377.
(43) Lee, C. T.; Yang, W. T.; Parr, R. G. *Phys. Rev. B* **1988**, *37*, 785−789.
(44) Diogo, H. P.; Ramos, J. J. M. *Phase Transit.* **2005**, *78*, 357−368.
(45) Nishikawa, K.; Tozaki, K.-i. *Chem. Phys. Lett.* **2008**, *463*, 369−372.
(46) Nishikawa, K.; Wang, S.; Tozaki, K.-i. *Chem. Phys. Lett.* **2008**, *458*, 88−91.
(47) Imanari, M.; Fujii, K.; Endo, T.; Seki, H.; Tozaki, K.-i.; Nishikawa, K. *J. Phys. Chem. B* **2012**, *116*, 3991−3997.
(48) Giraud, G.; Gordon, C. M.; Dunkin, I. R.; Wynne, K. *J. Chem. Phys.* **2003**, *119*, 464−477.

(49) Li, J.; Wang, I.; Fruchey, K.; Fayer, M. D. *J. Phys. Chem. A* **2006**, *110*, 10384−10391.
(50) Shirota, H.; Funston, A. M.; Wishart, J. F.; Castner, E. W. *J. Chem. Phys.* **2005**, *122*, 184512-1−184512-12.
(51) Fujisawa, T.; Nishikawa, K.; Shirota, H. *J. Chem. Phys.* **2009**, *131*, 244519-1−244519-14.
(52) Russina, O.; Triolo, A.; Gontrani, L.; Caminiti, R.; Xiao, D.; Hines, L. G., Jr.; Bartsch, R. A.; Quitevis, E. L.; Pleckhova, N.; Seddon, K. R. *J. Phys.: Condens. Mat.* **2009**, *21*, 424121-1−424121-9.
(53) Turton, D. A.; Hunger, J.; Stoppa, A.; Hefter, G.; Thoman, A.; Walther, M.; Buchner, R.; Wynne, K. *J. Am. Chem. Soc.* **2009**, *131*, 11140−11146.
(54) Shirota, H.; Fukazawa, H.; Fujisawa, T.; Wishart, J. F. *J. Phys. Chem. B* **2010**, *114*, 9400−9412.
(55) Turton, D. A.; Sonnleitner, T.; Ortner, A.; Walther, M.; Hefter, G.; Seddon, K. R.; Stana, S.; Plechkova, N. V.; Buchner, R.; Wynne, K. *Faraday Discuss.* **2012**, *154*, 145−153.
(56) Kinoshita, S.; Kai, Y.; Yamaguchi, M.; Yagi, T. *Phys. Rev. Lett.* **1995**, *75*, 148−151.
(57) Cho, M. H.; Du, M.; Scherer, N. F.; Fleming, G. R.; Mukamel, S. *J. Chem. Phys.* **1993**, *99*, 2410−2428.
(58) Kojima, S. *Phys. Rev. B* **1993**, *47*, 2924−2927.
(59) Sokolov, A. P.; Rossler, E.; Kisliuk, A.; Quitmann, D. *Phys. Rev. Lett.* **1993**, *71*, 2062−2065.
(60) Sokolov, A. P.; Kisliuk, A.; Quitmann, D.; Kudlik, A.; Rossler, E. *J. Non-Cryst. Solids* **1994**, *172*, 138−153.
(61) Cummins, H. Z.; Li, G.; Du, W. M.; Pick, R. M.; Dreyfus, C. *Phys. Rev. E* **1996**, *53*, 896−904.
(62) Yannopoulos, S. N.; Papatheodorou, G. N. *Phys. Rev. B* **2000**, *62*, 3728−3734.
(63) Grigera, T. S.; Martin-Mayor, V.; Parisi, G.; Verrocchio, P. *Nature* **2003**, *422*, 289−292.
(64) Ribeiro, M. C. C. *J. Chem. Phys.* **2010**, *133*, 024503-1−024503-6.
(65) Ribeiro, M. C. C. *J. Chem. Phys.* **2011**, *134*, 244507-1−244507-11.
(66) Le, M. L. P.; Alloin, F.; Strobel, P.; Lepretre, J.-C.; del Valle, C. P.; Judeinstein, P. *J. Phys. Chem. B* **2010**, *114*, 894−903.
(67) Siqueira, L. J. A.; Ribeiro, M. C. C. *J. Chem. Phys.* **2011**, *135*, 204506-1−204506-7.
(68) Urahata, S. M.; Ribeiro, M. C. C. *J. Chem. Phys.* **2004**, *120*, 1855−1863.
(69) Lopes, J.; Padua, A. A. H. *J. Phys. Chem. B* **2006**, *110*, 3330−3335.
(70) Annapureddy, H. V. R.; Kashyap, H. K.; De Biase, P. M.; Margulis, C. J. *J. Phys. Chem. B* **2010**, *114*, 16838−16846.
(71) Deetlefs, M.; Hardacre, C.; Nieuwenhuyzen, M.; Padua, A. A. H.; Sheppard, O.; Soper, A. K. *J. Phys. Chem. B* **2006**, *110*, 12055−12061.
(72) Russina, O.; Triolo, A. *Faraday Discuss.* **2012**, *154*, 97−109.
(73) Triolo, A.; Russina, O.; Fazio, B.; Appetecchi, G. B.; Carewska, M.; Passerini, S. *J. Chem. Phys.* **2009**, *130*, 164521-1−164521-6.
(74) Hayes, R.; Imberti, S.; Warr, G. G.; Atkin, R. *Phys. Chem. Chem. Phys.* **2011**, *13*, 13544−13551.
(75) Hayes, R.; Imberti, S.; Warr, G. G.; Atkin, R. *Phys. Chem. Chem. Phys.* **2011**, *13*, 3237−3247.
(76) Santos, C. S.; Annapureddy, H. V. R.; Murthy, N. S.; Kashyap, H. K.; Castner, E. W., Jr.; Margulis, C. J. *J. Chem. Phys.* **2011**, *134*, 064501-1−064501-10.
(77) Siqueira, L. J. A.; Ribeiro, M. C. C. *J. Phys. Chem. B* **2009**, *113*, 1074−1079.
(78) Paulechka, Y. U.; Blokhin, A. V.; Kabo, G. J.; Strechan, A. A. *J. Chem. Thermodyn.* **2007**, *39*, 866−877.
(79) Zak, Z.; Ruzicka, A.; Michot, C. *Z. Kristallogr.* **1998**, *213*, 217−222.
(80) Xue, L. X.; Padgett, C. W.; DesMarteau, D. D.; Pennington, W. T. *Solid State Sci.* **2002**, *4*, 1535−1545.